Journal of Power Sources 195 (2010) 674–679

Contents lists available at ScienceDirect

Journal of Power Sources

journal homepage: www.elsevier.com/locate/jpowsour

Self-supported supercapacitor membranes: Polypyrrole-coated carbon nanotube networks enabled by pulsed electrodeposition

Yueping Fang[a], Jianwei Liu[a], Deok Jin Yu[d], James P. Wicksted[d], Kaan Kalkan[e], C. Ozge Topal[e], Bret N. Flanders[b], Judy Wu[c], Jun Li[a,*]

[a] Department of Chemistry, Kansas State University, Manhattan, KS 66506, United States
[b] Department of Physics, Kansas State University, Manhattan, KS 66506, United States
[c] Department of Physics, University of Kansas, Manhattan, KS 66044, United States
[d] Department of Physics, Oklahoma State University, Stillwater, OK 74078, United States
[e] Department of Mechanical and Aerospace Engineering, Oklahoma State University, Stillwater, OK 74078, United States

ARTICLE INFO

Article history:
Received 10 June 2009
Received in revised form 14 July 2009
Accepted 15 July 2009
Available online 23 July 2009

Keywords:
Supercapacitor
Carbon nanotube film
Electrical conducting polymer

ABSTRACT

Self-supported supercapacitor electrodes with remarkably high specific capacitance have been developed by homogeneously coating polypyrrole (PPy) on multi-walled carbon nanotube (MWCNT) membranes. Polypyrrole can be deposited around the individual MWCNTs in a uniform manner throughout the MWCNT membrane via a pulsed electrochemical deposition method. This approach optimizes the pseudocapacitance of the membrane. Electrochemical data and Raman spectra indicate that the high specific capacitance is not only due to more uniform PPy coating, but also higher redox activity that is likely associated with a more ordered PPy packing. Such composite membranes can be directly used as supercapacitor electrodes without backing metal films or binders. A remarkable specific capacitance of 427 F g^{-1} has been achieved using 5-s electrodeposition pulses. This technique provides a viable solution for developing high-performance electrical energy storage devices.

1. Introduction

Accompanying the development of renewable energy technologies for electricity generation, efficient electrical energy storage (EES) techniques also become increasingly important [1,2]. Supercapacitors and batteries are currently the two major EES devices. Supercapacitors are desirable for applications requiring high power densities. Activated carbon has been commonly used in such applications with a specific capacitance (SC) as high as 125 F g^{-1} [3]. Recently, carbon nanotubes (CNTs), due to their high surface area, low electrical resistance, low mass density, and high stability, are recognized as attractive supercapacitor electrode materials. More importantly, high-aspect-ratio CNTs with the length over 10 μm behave as conductive wires that entangle with each other to form well interconnected networks. Networks of both single-walled CNTs (SWCNTs) and multi-walled CNTs (MWCNTs) have been investigated as electric double-layer capacitors (EDLCs). However, the SC varies from 4 to 135 F g^{-1}, strongly depending on the sample preparation and electric contact with the current collectors [4–6]. Electrically conductive polymers (ECPs) such as polypyrrole (PPy) have been deposited on carbon nanotubes to form composite materials with augmented capacitances due to the redox properties of the PPy [7–13]. The SC was indeed increased to ~190 F g^{-1} in most studies [14–16] with a few exceptions reporting much higher values [8]. The large variation was due to uncontrolled composite composition, film thickness, and poor contact with current collectors. Most studies have required metal backing foils and binders to ensure good electrical contact. These features added extra mass to the devices that was not considered in the SC determinations. For example, one study reported an exceptionally high SC of 890 F g^{-1} [8]. However, without knowing the MWCNT mass of the composite, one cannot make a reliable determination of the overall SC of the composite. In addition, the SC was measured with a PPy/MWCNT composite film deposited on a glassy carbon electrode which weighed many orders of magnitude higher than the composite itself. Such studies are not relevant to practical EES applications since the true SC value in a practical supercapacitor made with such materials is much lower if normalized to the overall electrode mass.

Self-supported composite sheets or films without backing electrodes are critical to improving electrical energy storage techniques. So far, most PPy/MWCNT supercapacitor materials show moderate SC value of ~131–191 F g^{-1} (with 1:1 SWCNT:PPy ratio) [16]. Here we report a new method to prepare freestanding MWCNT membranes with uniform PPy coatings that are self-supporting and

* Corresponding author. Tel.: +1 785 5320955; fax: +1 785 5326666.
E-mail address: junli@ksu.edu (J. Li).

0378-7753/$ – see front matter © 2009 Elsevier B.V. All rights reserved.
doi:10.1016/j.jpowsour.2009.07.033

can be used directly as supercapacitor electrodes without binders or backing metals. The structural homogeneity and capacitance of CNT-ECP composites are generally limited by the synthesis routes [15]. Electrodeposition on pre-assembled CNT membranes often blocks electrolyte channels at the outer surface while one-pot chemical co-polymerization with CNTs from solution suffers from ECP aggregation and high resistances due to poor CNT interconnection. Here we improve electrodeposition using well-separated short potential pulses and demonstrate that the uniformity of PPy coating can be significantly improved. This approach coats the individual MWCNTs with an ultrathin conformal PPy layer in a uniform manner throughout the whole membrane. As a result, the SC of the membrane has been increased to 427 F g^{-1} (normalized to the mass of CNTs).

2. Experimental

Sodium sulfate, potassium chloride and pyrrole (99%) were purchased from Thermo Fisher Scientific Inc. Purified multi-wall carbon nanotubes (MWCNTs) with outer diameters of 8–15 nm and lengths of ~50 μm were purchased from BuckyUSA Inc. Detailed analysis of the diameter distribution is shown in Fig. 2, which was obtained by measuring the diameters of carbon nanotubes from TEM images (Fig. 1).

The MWCNT membranes consisting of randomly stacked MWCNT networks were fabricated as follows: 2.0 ± 0.5 mg of MWCNTs were dispersed in 30 ml of absolute ethyl alcohol by sonicating for 2 h, then filtered through a filtration membrane (the diameter of 25 mm and pore size: 0.2 μm, Whatman) using a simple filtration flask and moderate vacuum by a water pump. The MWCNTs remain on the surface of the filtration membrane forming a flexible free-standing membrane with entangled internal networks. After drying at 50 °C under vacuum, the MWCNT membrane with the diameter of 2.0 cm and the thickness of ~50 μm is ready for use as an electrode without any further treatment.

A potentiostat (Parstat 2273 Analyzer, Princeton Applied Research Corporation) was used for electrochemical experiments. Electrochemical tests were conducted using a three-electrode setup. The working electrodes were the MWCNT membranes prepared by the procedures described above. A stainless steel (SS) ring with inner diameter of 16.5 mm, which was made of a SS wire with diameter of 0.75 mm, was placed around the outer edge of the circular MWCNT membrane and used as the current collector for the working electrodes. A Pt coil and a Ag/AgCl (sat'd KCl) electrode were used as the counter electrode and reference electrode for electrochemical deposition of polypyrrole (PPy) by a pulsed potentioamperometric method in aqueous solutions containing 50 mM pyrrole and 1.0 M KCl. The electrode potential was programmed with a waveform consisting of a potential step to 1.05 V (vs. Ag/AgCl

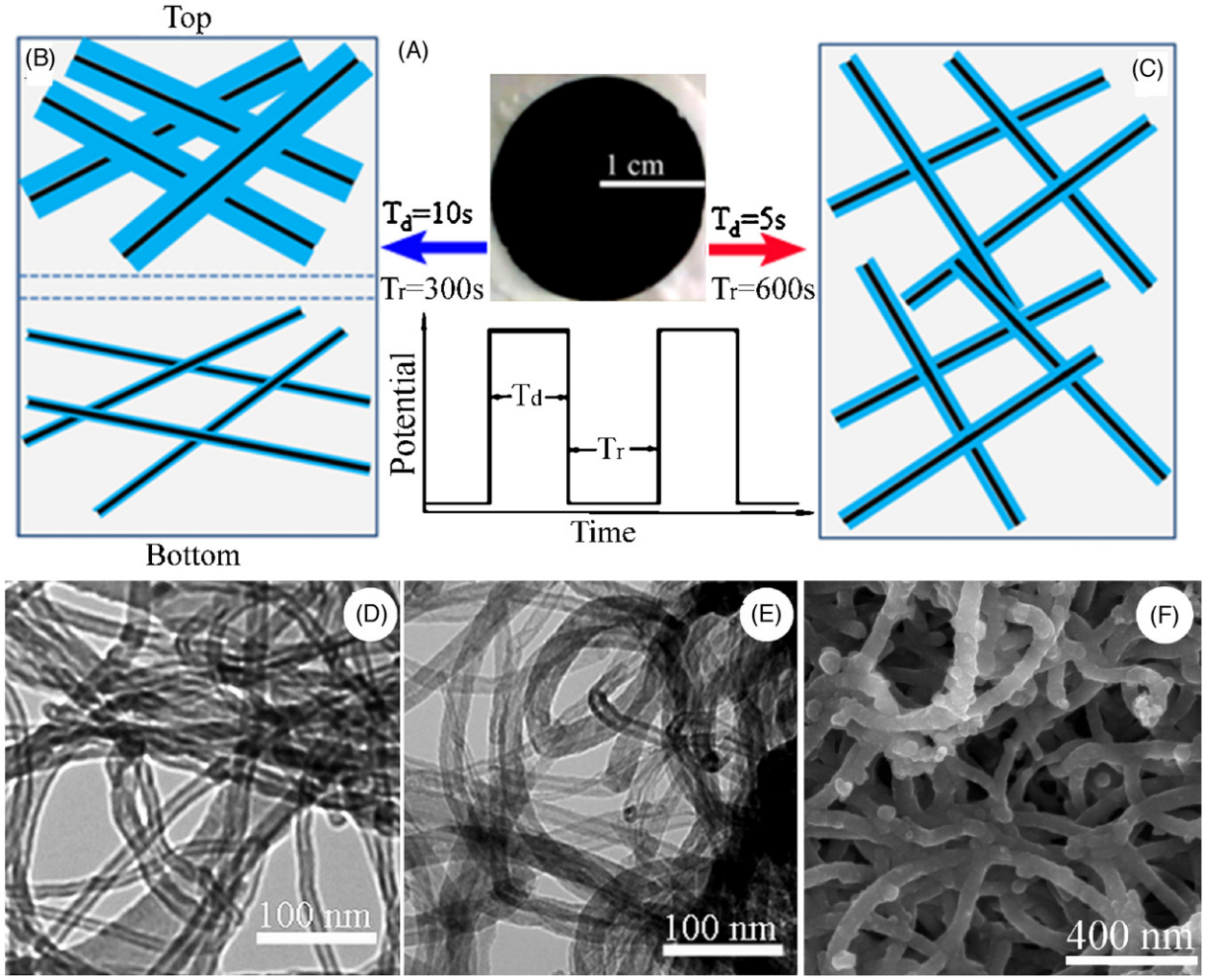

Fig. 1. (A) An optical image of MWCNT membrane with the diameter of 20 mm on a filtration membrane (top panel) and an illustration of the electropotential waveform for pulsed PPy electrodeposition (bottom panel). (B) and (C) Schematic of the PPy coating on MWCNTs under T_d = 10 s, T_r = 300 s and T_d = 5 s, T_r = 600 s, respectively. (D) A TEM image of the pure MWCNTs. (E) A TEM image of the MWCNTs after a total of 70 s PPy deposition with repeated pulses of T_d = 5 s and T_r = 600 s. (F) An SEM image of the top surface of the MWCNT membrane after PPy deposition for 70 s under T_d = 5 s and T_r = 600 s.

(sat'd KCl)) for the deposition time T_d followed by cell off at a rest time T_r (see Fig. 1). This waveform can be repeated until the desired amount of PPy is obtained, which is indicated by the total charge Q obtained by integrating the deposition current over time. The background current is measured by applying the same waveform in a solution with 1.0 M KCl but without pyrrole, as shown in Fig. 3.

Cyclic voltammetry (CV) in three-electrode setup was used to characterize the supercapacitance of MWCNT membranes before and after coating with PPy films. A stainless steel mesh (size: 2 cm × 2 cm) and 1.0 M Na_2SO_4 aqueous solution were used as the counter electrode and the electrolyte. Specific capacitance (SC) of the working electrodes was calculated from CV measurements in the potential range from −0.40 to +0.60 V (vs. Ag/AgCl (sat'd KCl)) based on the formula $SC = (Q_a + |Q_c|)/2m_{CNT}\Delta E)$, where Q_a and Q_c are the anodic and cathodic charge in respective scans; m_{CNT} is the mass of MWCNTs; and ΔE is the potential range of the CV scans.

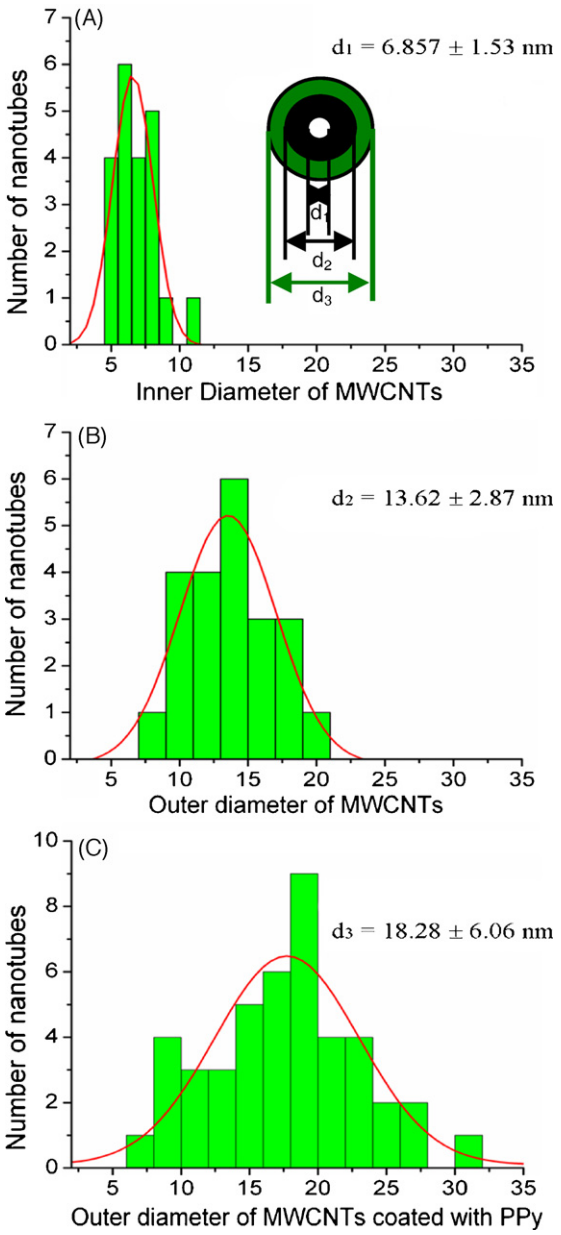

Fig. 2. Histograms of diameter distributions: (A) inner diameters (d_1) of the pure MWCNTs; (B) outer diameters (d_2) of the pure MWCNTs; (C) outer diameters (d_3) of the MWCNTs after the deposition of PPy for 70 s under T_d = 5 s and T_r = 600 s.

The microstructure of the composite electrodes was observed by means of scanning electron microscopy (SEM) (Hitachi VP-SEM S-3400N) and transmission electron microscopy (TEM) (FEI CM100). Raman spectra were collected across the 500–2000 cm^{-1} region with a CCD-detector-based Raman microscope (Renishaw) using the 514.5 nm line of an Ar^+ laser as its excitation source. This beam delivered 5 mW of power to a ~10 μm diameter spot on the sample.

3. Results and discussion

Fig. 1A shows a MWCNT membrane with the diameter of 20 mm and thickness of ~50 μm (top panel), which was fabricated by dispersing 2.0 ± 0.5 mg of MWCNTs in absolute ethanol, passing the

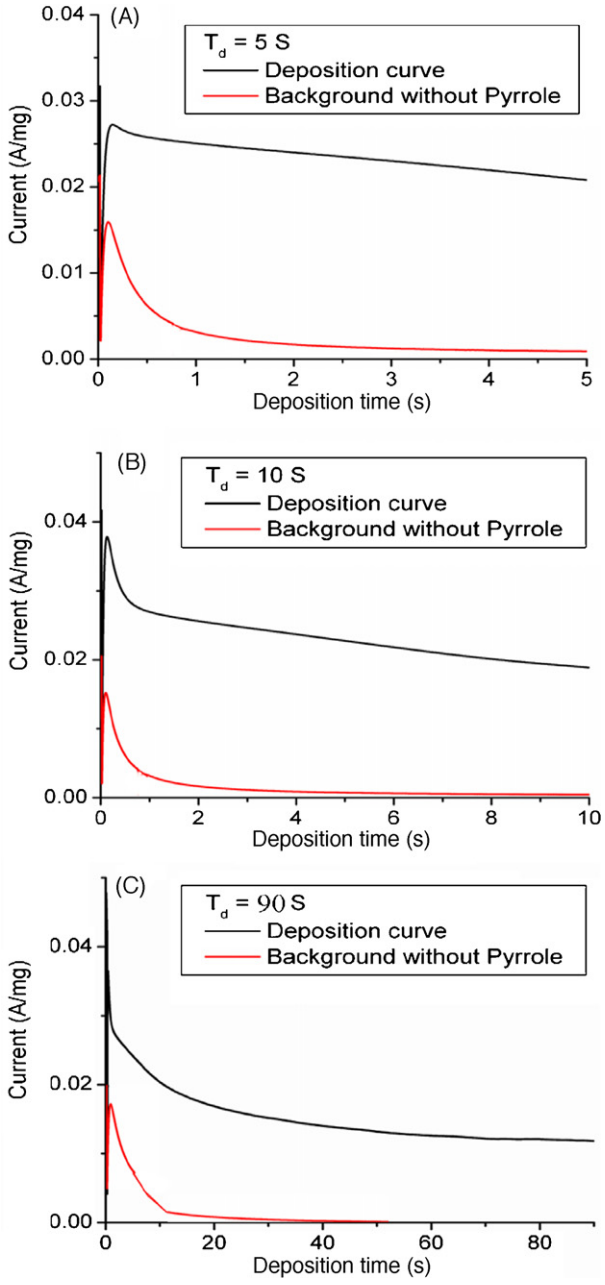

Fig. 3. The current–time curves for the deposition of PPy on MWCNT membranes under three different conditions: (A) T_d = 5 s and T_r = 600 s, (B) under T_d = 10 s and T_r = 300 s and (C) under T_d = 90 s and T_r = 0 s. All red curves are the background current with the same potential waveform in absence of pyrrole. (For interpretation of the references to color in this figure caption, the reader is referred to the web version of the article.)

solution through a filtration membrane and then drying the membrane in vacuum. The bottom panel illustrates the waveform of electropotential (E) applied at the MWCNT membrane for pulsed electrodeposition of PPy from 50 mM pyrrole in 1.0 M KCl aqueous electrolyte. During the deposition time T_d, E is held at 1.05 V vs. Ag/AgCl (sat'd KCl) for electropolymerization and the cell is at open circuit during the resting time T_r. Such potential waveforms are repeated until the desired amount of PPy is deposited. The resting time allows more pyrrole monomers in the bulk solution to diffuse into the space between carbon nanotubes throughout the MWCNT membrane before the next deposition pulse. Under $T_d = 10$ s and $T_r = 300$ s, thicker PPy coating is obtained at the top surface and thinner coating at the back side of the membrane (Fig. 1B).

Under $T_d = 5$ s and $T_r = 600$ s, a more homogeneous PPy coating is obtained over the entire membrane (Fig. 1C). Fig. 1D and E shows TEM images of the MWCNTs before and after PPy deposition. The pure MWCNTs have the outer diameter d_2 varying between 8 and 20 nm. After a total deposition time of 70 s under $T_d = 5$ s and $T_r = 600$ s, the outer diameter d_3 of the PPy-coated MWCNT is increased to 7–32 nm. The distributions are fit with Gaussian functions (Fig. 2) with mean and standard deviation values of inner diameter $d_1 = 6.88 \pm 1.53$ nm and outer diameter $d_2 = 13.62 \pm 2.87$ nm for pure MWCNTs, and of outer diameter $d_3 = 18.28 \pm 6.06$ nm after coating with PPy. From these data, the average thickness of the PPy coating is estimated to be ~2.3 nm for this sample. The SEM image in Fig. 1F shows that the PPy coating conforms to the nanotubular structure of the membrane's top surface and that the nanoscale space between the tubes has remained open throughout the coating process, allowing electrolyte to fill the internal spaces of the membrane.

An important performance feature of an individual membrane is the PPy-quantity Q that was deposited on it. Q is found by integrating the PPy deposition current (Fig. 3A–C) over each deposition cycle of period T_d. As Fig. 4A shows, the PPy deposition profiles are linearly proportional to the total deposition time, i.e. $Q \propto N \times T_d$ with N = number of repeated cycles. Interestingly, the red profile which corresponds to the shortest deposition pulses (5 s) has the largest slope, indicating more effective PPy deposition; this behavior is likely because more pyrrole monomers can access the space between carbon nanotubes inside the MWCNT membrane when $T_d = 5$ s and $T_r = 300$ s are used. The vertical lines labeled b, c, and d denote specific PPy-quantities, i.e. Q, that were deposited under continuous, long-pulsed ($T_d = 10$ s), and short-pulsed ($T_d = 5$ s) deposition, respectively. These specific membranes will be referred to further. We characterize the SC of each membrane by measuring a CV profile of the membrane. Fig. 4B shows the CV profiles of membranes b, c, and d, as well as a PPy-free MWCNT membrane denoted membrane a. The sum of the anodic and cathodic charges ($Q_a + |Q_c|$) is proportional to the SC of the membrane, as given by $SC = (Q_a + |Q_c|)/2m_{CNT}\Delta E$. These sums are extracted from the CV profiles of the individual films by integrating around their $I(V)$ loops.

$$Q_a + |Q_c| = \oint \frac{I(V)}{\nu} dV \quad (1)$$

where the voltage scan rate is $\nu = 5$ mV s^{-1}. The CV-profiles of films a, b, c, and d are shown in Fig. 4B. Fig. 4C plots the SC values of membranes prepared with 5 s deposition pulses (red triangles), 10 s deposition pulses (blue points), 90 s of continuous deposition (filled

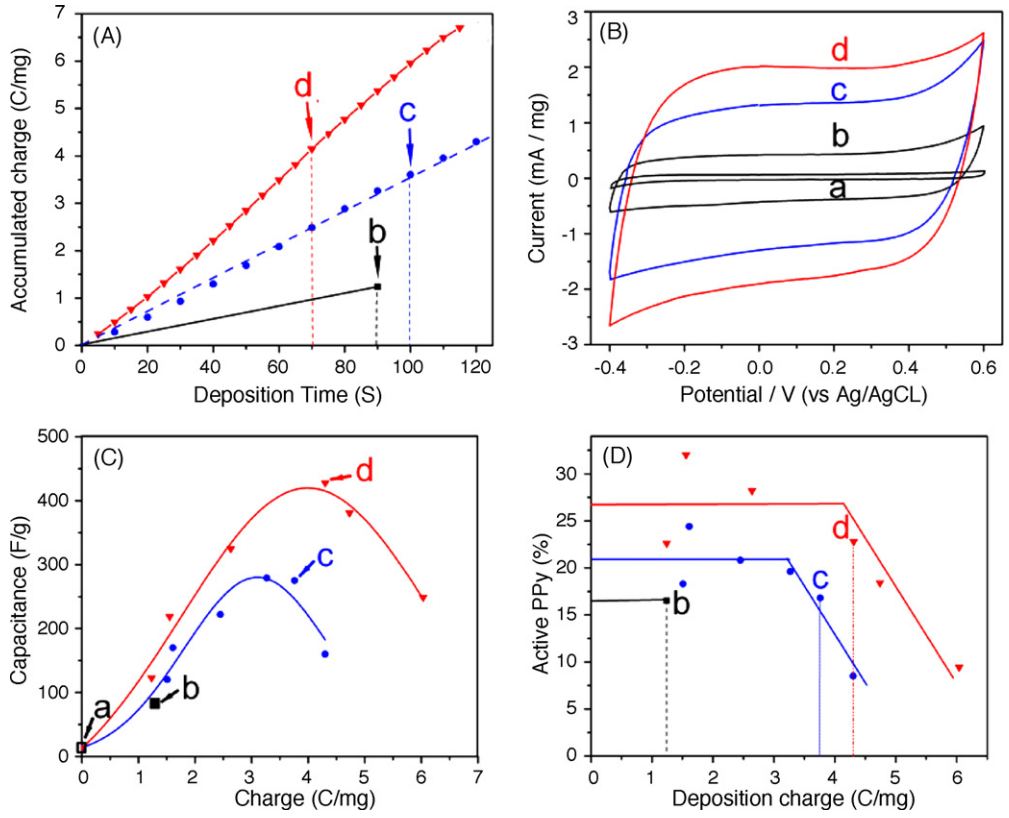

Fig. 4. (A) The total PPy deposition charge vs. the total deposition time at $T_d = 90$ s, $T_r = 0$ (black line); $T_d = 10$ s, $T_r = 300$ s (blue line); and $T_d = 5$ s, $T_r = 600$ s (red line). (B) Cyclic voltammograms of four samples represented by points a, b, c, d in panel C in 1.0 M Na_2SO_4 at a scan rate of 5 mV s^{-1}. (C) The specific capacitance vs. the total charge of PPy deposition on the MWCNT membranes. Both quantities are normalized to the mass of MWCNTs. The PPy was deposited under pulsed electrodeposition conditions at $T_d = 5$ s, $T_r = 600$ s (red curve); and $T_d = 10$ s, $T_r = 300$ s (blue curve). Point a is from a pure MWCNT membrane and point b is from a MWCNT membrane after 90 s continuous PPy deposition. (D) The percentage of redox-active PPy during CV cylcles vs. total PPy (represented by the integrated deposition charges). (For interpretation of the references to color in this figure caption, the reader is referred to the web version of the article.)

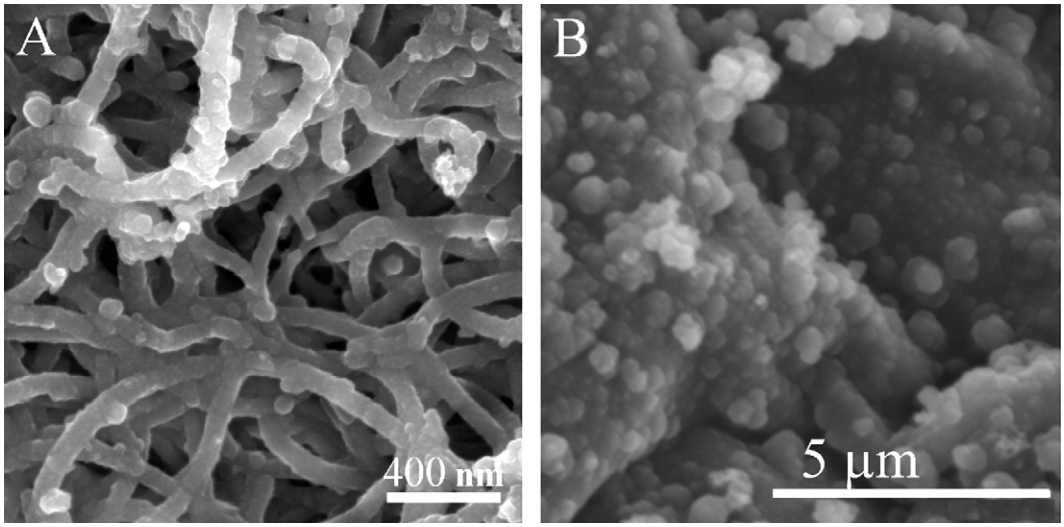

Fig. 5. SEM image of MWCNT networks after deposition of PPy under T_d = 5 s and T_r = 600 s: (A) for 70 s (corresponding to point d in Fig. 2(A)) and (B) for 120 s.

square), and with no PPy at all (hollow square), vs. Q, the amount of PPy that was deposited on each of the membranes. The SC values and the Q values were normalized by the MWCNT mass (~2.0 mg).

The MWCNT membrane is electrically connected with a 0.75 mm diameter stainless steel ring around the edge. Fig. 4C shows that the pure MWCNT membrane has a SC of ~13 F g^{-1} (point a). After continuous PPy deposition for 90 s, the SC increases to 87 F g^{-1} (point b), slightly lower than that reported in the literature [3–10] due to the absence of metal backing films and binders in our samples. Nevertheless, by using pulsed electrodeposition, the SC value is dramatically increased as more PPy is deposited (blue and red lines). Maximum SC values of 275 F g^{-1}(point c in Fig. 4C) and 427 F g^{-1} (point d in Fig. 4C) can be obtained with deposition-parameters of T_d = 10 s, T_r = 300 s and of T_d = 5 s, T_r = 600 s, respectively. The SC value drops if the PPy deposition is over ~3.2 C mg^{-1} for T_d = 10 s and ~4.3 C mg^{-1} for T_d = 5 s.

Clearly, the SC value can be increased over 30 times if PPy is deposited properly. In general, short T_d allows monomers to diffuse from the bulk solution into the space between carbon nanotubes inside the membrane and thus produces more uniform PPy coating. Long T_d, on the other hand, results in much thicker PPy coating at the exterior than that at interior of the MWCNT membrane. The clogging of the space between carbon nanotubes at the membrane exterior is found to lower the SC value. As a result, the same amount of PPy that is deposited at shorter T_d gives higher SC than at longer T_d conditions. Even for shorter T_d, the exterior membrane will be clogged if the amount of PPy significantly exceeds the optimum value (point d in Fig. 4C), as shown by the SEM images in Fig. 5.

The mass of deposited PPy (m_{PPy}) can be estimated from the deposition charge Q using $Q = n_e F m_{PPy}/M_{Py}$, where n_e = 2.30 accounts for 2.30 electrons per pyrrole during electrodeposition to form the partially oxidized PPy (0.30 e more than the required 2e for forming native PPy) [17], as schematically shown below:

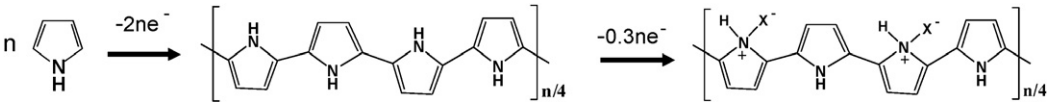

(2)

F is the Faradaic constant and M_{Py} = 65.05 g mole^{-1} is the molar mass of the pyrrole unit in the polymer chain. For point d in Fig. 4A, the deposition charge Q = 4.30 C mg^{-1} leads to ~1.26 mg of PPy on a 1.0 mg MWCNT membrane. With the mass ratio defined as in Eq. (3).

$$\frac{m_{PPy}}{m_{CNT}} = \frac{\rho_{PPy} V_{PPy}}{\rho_{CNT} V_{CNT}} = \frac{\rho_{PPy}(d_3^2 - d_2^2)}{\rho_{CNT}(d_2^2 - d_1^2)} = 1.26 \quad (3)$$

where the density of PPy is ρ_{PPy} = 1.50 g cm^{-3} and the density of the graphitic MWCNT sidewall is assumed to be the same as graphite, i.e. ρ_{CNT} = 2.1 g cm^{-3}, the PPy thickness can be calculated as $(d_3 - d_2)/2$ = ~3.5 nm, ~50% larger than the 2.3 nm average PPy thickness estimated from TEM images in Fig. 1D and E. The main error is likely due to the fact that the electron transfer per pyrrole is more than 2.30 e (i.e. n_e > 2.30) during electrodeposition of PPy because the electropotential was held at the high oxidation potential (1.05 V vs. Ag/AgCl (sat'd KCl)). Part of the PPy is reduced back to the lower oxidation state (resulting in an overall n_e = 2.30) when the potential is lowered for SC analysis and other measurements.

Despite the large error, the above calculation gives us a necessary estimation of how much PPy might be deposited. The exact amount of PPy deposited on the MWCNT membrane was difficult to directly measure in our experiments due to two reasons: first, in most experiments the mass of deposited PPy is much less than that of MWCNTs in the membrane; second, the wet film after deposition makes the measurement of such small mass change unreliable. Due to these reasons, we only report our results in Fig. 4 as those normalized to the dry mass of MWCNTs before it is submerged in the solution. This may cause the SC value to be higher than the true value which should include that of PPy. However, our estimation with a worst case-scenario calculation indicates that the difference will be less that a factor of 2. Therefore the SC value after including this factor will still be higher than previous reports.

The integrated anodic charge Q_a or cathodic charge Q_c represents how much PPy can be further oxidized or reduced during CV. After normalizing to the total electrodeposition charge Q, the redox active PPy content at various deposition conditions appears to be only ~16–27% (Fig. 4D), i.e. only ~16–27% deposited pyrrole unit is oxidized and reduced to generate pseudocapacitance in each CV cycle. We only use a small portion of the supercapacitor capacity in CV between −0.4 and +0.60 V. Importantly, the active PPy con-

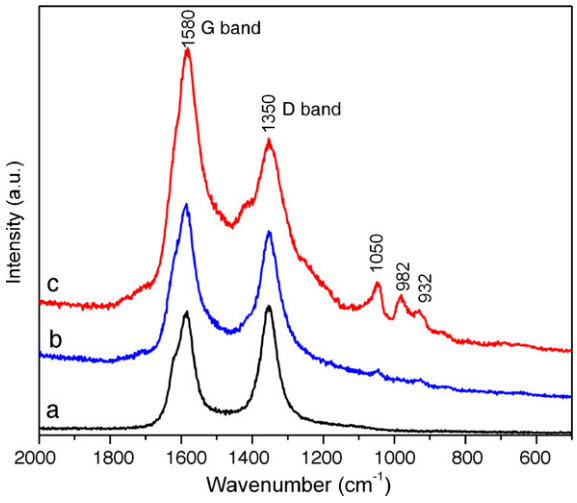

Fig. 6. Raman spectra of (a) a pure MWCNT membrane (black line), (b) a MWCNT membrane after 90 s continuous PPy deposition (blue line), and (c) a MWCNT membrane after deposition of PPy for 70 s using T_d = 5 s and T_r = 600 s (red line). (For interpretation of the references to color in this figure caption, the reader is referred to the web version of the article.)

tent at the initial stage is higher when shorter deposition pulse T_d is applied, indicating the improved homogeneity and higher PPy quality. Under each deposition condition, the active PPy content remains constant at low deposition, but decreases linearly if the deposition is over the threshold corresponding to the maxima c and d in Fig. 4C. Shorter deposition pulse followed by a sufficient resting time for diffusion gives both of a higher initial active PPy content and a higher transition threshold, thus resulting in a higher SC value at the maximum condition. The ability for fast electrodeposition using short pulses is likely due to the strong π–π stacking of pyrrole or PPy backbone on the graphitic sidewall of MWCNTs [18]. Fig. 1E and F clearly shows the preferential adhesion and structural uniformity of PPy coating on MWCNT enabled by the short-pulsed electrodeposition. The SC value of PPy films deposited with both 5 and 10 s pulses shows a maximum and then decreases as more PPy is deposited. This may be attributed to two reasons: first, the open space between CNTs at the exterior membrane surface may be partially filled and thus blocks the electrolyte access to interior of the CNT membrane when PPy deposition exceed certain amounts; (as shown in Fig. 5) second, the activity of the PPy may drop and PPy becomes more disordered as thicker PPy film is deposited around each CNT.

To further understand the structure of the PPy film deposited on MWCNT surface, we employed Raman spectroscopy. Fig. 6 shows Raman spectra from three samples: (1) a pure MWCNT membrane, (2) a MWCNT membrane after 90 s continuous PPy deposition, and (3) a MWCNT membrane after deposition of PPy for 70 s using pulse electrodeposition, i.e. T_d = 5 s and T_r = 600 s. The most prominent features are the D band (at ~1350 cm^{-1}) and G band (at ~1580 cm^{-1}) from MWCNTs. The ratio of D band to G band is associated with the extent of defects present in the MWCNTs and is sensitive to the molecular interaction at the interface between PPy and MWCNT [19]. After PPy deposition, particularly with the short-pulsed deposition method, the D/G ratio decreased, indicating the reduction of disordering at the MWCNT surface. More interestingly, only the PPy-CNT sample deposited with short pulses (T_d = 5 s) shows additional features in the range of 900–1100 cm^{-1}. These may be attributed to the PPy ring deformation (at 982 and 932 cm^{-1}) and C–H in-plane bending (at ~1050 cm^{-1}) of dications (bipolaron) and radical cations (polaron). The evident polaron and bipolaron intensity indicates the high electric conductivity [20,21] likely due to the more ordered PPy packing on MWCNT surface enabled by the strong π–π stacking between PPy conjugate backbone and graphitic sidewall of MWCNTs. PPy deposition with short pulses allows the polymer backbone to rearrange to form more ordered structure. Both the structural uniformity and high conductivity of PPy coating help to provide higher pseudocapacitance in this application.

4. Conclusions

In summary, the pulsed electrodeposition technique enables growth of a much more homogeneous and electrochemically active MWCNT-PPy composite membrane. This allows the internal space between MWCNTs to be accessed by electrolytes, giving an enhanced SC. The composite membrane can be directly used as self-supported supercapacitor electrodes without backing films and binders. The SC is as high as ~427 F g^{-1} in a mild neutral electrolyte (i.e. 1 M Na_2SO_4). Further optimization of the electrode connection and the use of more active ECPs such as polyaniline [14,22] may readily lead to useful high-performance EES devices.

References

[1] DOE Workshop Report on Basic Research Needs for Electrical Energy Storage, 2007.
[2] A.S. Arico, P. Bruce, B. Scrosati, J.M. Tarascon, W. Van Schalkwijk, Nat. Mater. 4 (2005) 366.
[3] J. Gambya, P.L. Tabernaa, P. Simon, J.F. Fauvarquea, M. Chesneaub, J. Power Sources 101 (2001) 109.
[4] E. Frackowiak, K. Metenier, V. Bertagna, F. Beguin, Appl. Phys. Lett. 77 (2000) 2421.
[5] M. Kaempgen, J. Ma, G. Gruner, G. Wee, S.G. Mhaisalkar, Appl. Phys. Lett. 90 (2007) 264104.
[6] C.G. Liu, M. Liu, F. Li, H.M. Cheng, Appl. Phys. Lett. 92 (2008) 143108.
[7] E. Frackowiak, V. Khomenko, K. Jurewicz, K. Lota, F. Beguin, J. Power Sources 153 (2006) 413.
[8] X.Q. Lin, Y.H. Xu, Electrochim. Acta 53 (2008) 4990.
[9] M. Hughes, M.S.P. Shaffer, A.C. Renouf, C. Singh, G.Z. Chen, J. Fray, A.H. Windle, Adv. Mater. 14 (2002) 382.
[10] C. Peng, J. Jin, G.Z. Chen, Electrochim. Acta 53 (2007) 525.
[11] G.Z. Chen, M.S.P. Shaffer, D. Coleby, G. Dixon, W.Z. Zhou, D.J. Fray, A.H. Windle, Adv. Mater. 12 (2000) 522.
[12] M. Gao, S.M. Huang, L.M. Dai, G. Wallace, R.P. Gao, Z.L. Wang, Angew. Chem. Int. Ed. 39 (2002) 3664.
[13] T. Mirfakhrai, J.D.W. Madden, R.H. Baughman, Mater. Today 10 (2007) 30.
[14] V. Khomenko, E. Frackowiak, F. Beguin, Electrochim. Acta 50 (2005) 2499.
[15] M. Hughes, G. Chen, M. Shaffer, D. Fray, A. Windle, Chem. Mater. 14 (2002) 1610.
[16] (a) J.Y. Oh, M.E. Kozlovc, B.G. Kima, H.K. Kim, R.H. Baughman, Y.H. Hwang, Synth. Met. 158 (2008) 638;
(b) E. Frackowiak, F. Beguin, Carbon 40 (2002) 1775.
[17] S. Sadki, P. Schottland, N. Brodie, G. Sabouraud, Chem. Soc. Rev. 29 (2000) 283.
[18] R.J. Chen, Y.G. Zhang, D.W. Wang, H.J. Dai, J. Am. Chem. Soc. 123 (2001) 3838.
[19] A.B. Dalton, C. Stephan, J.N. Coleman, B. McCarthy, P.M. Ajayan, S. Lefrant, P. Bernier, W.J. Blau, H.J. Byrne, J. Phys. Chem. B 104 (2000) 10012.
[20] J. Mikat, I. Orgzall, H.D. Hochheimer, Synth. Met. 116 (2001) 167.
[21] J. Mikat, I. Orgzall, H.D. Hochheimer, Phys. Rev. B 65 (2002) 174202.
[22] V. Gupta, M. Norio, Electrochim. Acta 52 (2006) 1721.